A Summary of the Fatigue Properties of Wind Turbine Materials

by

Herbert J. Sutherland
Sandia National Laboratories
Wind Energy Technology Department
Albuquerque, New Mexico 87185-0708

Abstract

Modern wind turbines are fatigue critical machines that are typically used to produce electrical power from the wind. The materials used to construct these machines are subjected to a unique loading spectrum that contains several orders of magnitude more cycles than other fatigue critical structures, e.g., an airplane. To facilitate fatigue designs, a large database of material properties has been generated over the past several years that is specialized to materials typically used in wind turbines. In this paper, I review these fatigue data. Major sections are devoted to the properties developed for wood, metals (primarily aluminum) and fiberglass. Special emphasis is placed on the fiberglass discussion because this material is current the material of choice for wind turbine blades. The paper focuses on the data developed in the U.S., but cites European references that provide important insights.

DISCLAIMER

DISCLAIMER

Portions of this document may be illegible in electronic image products. Images are produced from the best available original document.

INTRODUCTION

Somewhat over two decades ago, utility grade wind turbines were designed using static and quasi-static analyses. At best, these rather simple analyses led to over-designed turbines, and at worst, they led to premature failures. The latter is exemplified by high failure rates observed in the early California wind farms. We, as designers, soon realized that wind turbines were *fatigue critical machines*; namely, the design of many of their components is dictated by fatigue considerations. And, not only is this machine fatigue critical, its unique load spectrum greatly exceeds our previous experience. This realization led to a large quantity of research that has now matured to the extent that state-of-the-art designs can include detailed fatigue analyses of the wind turbine. In a recent paper, Sutherland[1] reviews these developments and describes the "best practices" for the fatigue analysis of wind turbine components. A major section of this report examines the recent research into the fatigue properties of typical wind turbine materials. This paper draws upon that work to develop a summary of the research into the fatigue properties of typical wind turbine materials. The paper focuses on U.S. technology but cites European references that provide important insights. An excellent summary of the European data is provided by Kensche.[2]

Wind Turbine Materials

Most of the materials used in the construction of wind turbines are typical of those materials that are used in rotating machinery and towers. Thus, the turbine system is primarily composed of materials that are relatively common structural materials with extensive engineering applications and databases. However, blades are unique structural components of wind turbines. They are a minimum weight and cost component that must endure a very large number of fatigue cycles during their service lifetime. As shown in Fig. 1, blades must endure several orders of magnitude more cycles than an airplane, the original fatigue critical structure. Thus, turbine blades are also fatigue critical structures. Moreover, the cost of the materials used in the turbine must be kept at a relative minimum to ensure a commercially viable product.

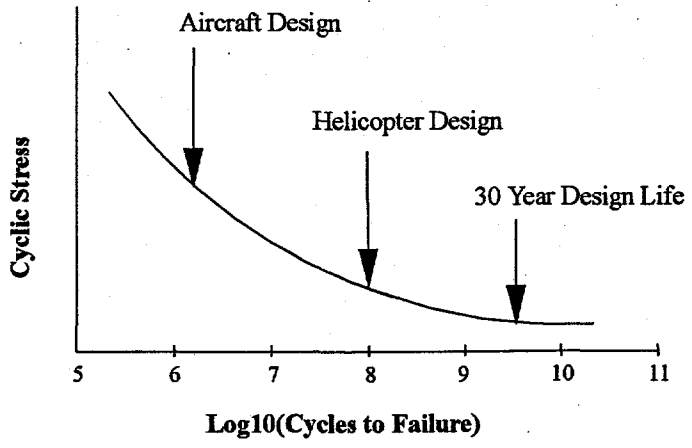

Figure 1. Schematic S-N Diagram for Various Fatigue Critical Structures.

Wind turbine blades have been made from a variety of materials that range from wood to metals to composites. Wood (a naturally occurring composite material) has proven to be a successful material. Its relatively high strength-to-weight ratio, and good stiffness and resilience yield high quality blades. Wood was used in the early windmills (including the early

Dutch windmills and the U.S. water pumpers) and has remained a favorite with the designer of small and medium sized wind turbines. However, wood's inherent problems with moisture stability and joining efficiency[3] have forced designers to examine other materials. Metals were initially a popular material because they yield a low-cost blade and can be manufactured with a high degree of reliability. However, most metallic blades (steel) proved to be relatively heavy, which limits their application in commercial turbines. Lightweight metals (aluminum) have found some applications. Composites have become the blade material of choice. High strength and stiffness and the ability to tailor the material to the loads has led to its widespread use as a blade material.

The bulk of the fatigue properties developed for materials that are used in wind turbine components are based on coupon tests conducted under constant amplitude loading. The techniques used in these tests have varied widely. Swanson[4] provides a general reference for typical testing techniques.

Characterization of Fatigue Properties

Typically, the fatigue characteristics of materials are determined by subjecting test specimens to fatigue cycles and counting the number of cycles to failure. In constant-amplitude fatigue tests, the data are typically called S-N data, reflecting the number of cycles, N, at the stress (or strain) level S required to fail the sample. For crack propagation the data, normally called da/dn data, track the number of cycles required to extend a crack of length a by a length da. In both cases, experimental procedures lend themselves to tracking the cycles to failure as a function of the cyclic amplitude while holding the mean or R ratio constant. (the R ratio for a fatigue cycle is defined as the ratio of the minimum stress in the cycle to the maximum). This testing procedure yields a family of curves that describes the fatigue behavior of the material.

The information contained in these curves is typically characterized using several standard techniques. The first and foremost is a presentation of the family of S-N curves themselves. This simple presentation can be somewhat deceiving, because various authors use various forms of S and n. In particular, the value of S can be chosen to be the range of the cycle, the amplitude of the cycle, the maximum of the cycle (tension) or the minimum of the cycle (compression). Moreover, these values may be normalized by ultimate tensile or compressive strength. The number of cycles n is usually the number of full cycles to failure. But it can also be the number of "cross-overs" (zero-crossings) or the number of reversals (two reversals for each full cycle). *Thus, one must also be cautious with S-N data. Always check the reference to ascertain the definitions of the variables used to characterize the data.*

In addition to the presentation of the family of curves, several other graphical and mathematical descriptions of the data have proven useful. A very popular graphical technique is the constant-life Goodman Diagram, and log-linear and log-log curve fitting techniques. This section of the paper discusses several of these techniques.

Goodman Diagram

For design, a family of S-N curves is typically not very useful. Rather, the designer prefers constant-life curves that depict the locus of all stress states that produce a given fatigue life. These curves allow the designer to determine quickly and accurately the effect on lifetime of changes in the stress or strain in a component under design.[5] A typical Goodman diagram is illustrated in Fig. 2. In this figure, the vertical axis is a measure of the cyclic amplitude, and the horizontal axis is a measure of the mean stress. In both cases, theses stress levels have been normalized by the ultimate tensile strength of the material.

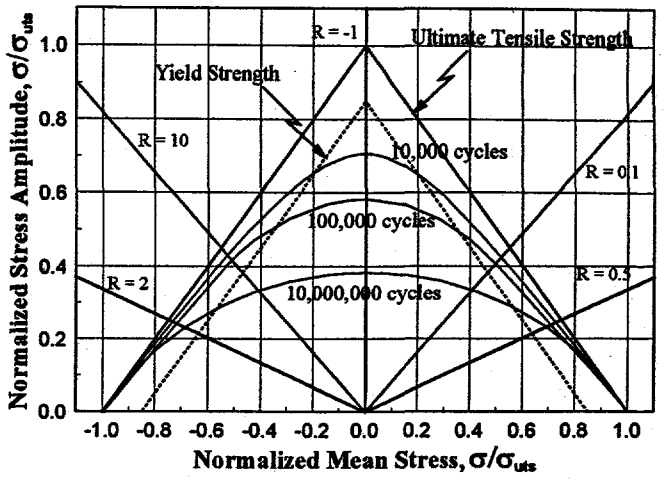

Figure 2. Typical Symmetric Goodman Diagram.

Figure 2 illustrates that a constant R ratio plots as a straight line in this diagram. All constant R ratio plots have their origin at zero mean and zero amplitude. Fully reverse bending, R = -1, is the vertical axis; i.e., the mean stress is zero.

In this figure, the constant life curves are bounded by the ultimate tensile strength of the material on the tensile side (right side) of the diagram. This stress level plots as a straight line between (0,1) and (1,0). Likewise, the ultimate compressive strength bounds the compressive side of diagram (left side). It plots between (0,1) and (-1,0). Similar straight lines are shown in the figure for the tensile and compressive yield stress. In this illustration, we assumed that the tensile and compressive strengths are equal.

Three representative constant life diagrams are shown in this figure, at 10,000, 100,000 and 10,000,000 cycles. Each constant-life plot can be constructed from a family of S-N curves. Depending on the data behind the plot, the constant-life curve may be straight-line segmented curve or a smooth fitted curve.

This diagram illustrated in Fig. 2 is called symmetric; namely the left side of the plot is the mirror image of the right side of the plot. Thus, for symmetric materials, the ultimate tensile and compressive strength must be equal, and fatigue life is dependent on the absolute value of the mean stress. For symmetric materials, only the right half of the full Goodman diagram is typically plotted. Metals are typically symmetric materials; fiberglass materials typically are not.

General Characterizations of Fatigue Behavior

Curve Fitting S-N Data

As discussed by many authors, the S-N behavior of composite materials at a constant R value is typically fit using one of two equations. The first is a power law of the form:

$$\sigma = CN^{1/m} = CN^{1/k} \quad , \tag{1}$$

or alternately,

$$\log(\sigma) = \log(C) + \frac{1}{m}\log(N) \quad , \tag{2}$$

where N is the number of cycles to failure at stress level σ, and the coefficient m, sometimes denoted by k or b, is called the fatigue exponent. In this form, *the fatigue exponent is a negative number; i.e., the stress level decreases as the number of cycles increases. However, most fatigue literature reports positive fatigue exponents; namely, Eqs. 1 and 2 have been rewritten with an explicit negative sign.* Thus, these two equations become:

$$\sigma = CN^{-1/m} = CN^{-1/k} \quad , \tag{3}$$

$$\log(\sigma) = \log(C) - \frac{1}{m}\log(N) \quad . \tag{4}$$

In nondimensional form, Eq. 3 takes the form:

$$\frac{\sigma}{\sigma_o} = C'N^{-1/m} = C'N^{-1/k} \quad , \tag{5}$$

or

$$\log\left(\frac{\sigma}{\sigma_o}\right) = \log(C') - \frac{1}{m}\log(N) \quad , \tag{6}$$

where σ_o is the static strength of the composite. In this form, C' *has a value of 1* when the curve fit to the S-N data set passes through the static strength at 10^0 cycles, i. e., at static failure in the first fatigue cycle. However, best fits for many materials yield values for C that are typically much larger than one. Thus, a multi-segmented curve is typically required to characterize the low and high cycle fatigue behavior of composites. For wind turbine applications where design lifetimes are relatively long, this region of the curve is typically not important.

The second form is given by a log-linear function of the form:

$$\sigma = C - \frac{1}{m}\log(N) = C - b\log(N) \quad , \tag{7}$$

or alternately,

$$10^{\sigma} = CN^{-1/m} \quad , \tag{8}$$

where the inverse of m is typically denoted by b. In nondimensional form, Eq. 7 takes the following form:

$$\frac{\sigma}{\sigma_o} = C' - \frac{1}{m}\log(N) = C' - b\log(N) \quad . \tag{9}$$

In this form, *C' also has a value of 1* when the curve fit to the S-N data set passes through the static strength at 10^0 cycles. Best fits typically yield values of C that are very close to one.

The exponent m in Eqs. 6 and 9 is different. When a specific S-N data set is fit with these two equations, the respective fatigue exponents are comparable, but they typically will not have the same magnitude. However, when used in damage analysis for spectral loads, the two fits produce significantly different predicted lifetimes.

Goodman Fit for Mean Stress

As discussed in preceding section, the family of S-N curves may be formed into the Goodman diagram shown in Fig. 2. For many materials, the dependence of the constant-life curves on alternating and mean stress may be collapsed into a single curve using a Goodman fit;[6] i.e., the Goodman diagram is mapped into a single curve that is based on an equivalent stress level. Typically, the data are collapsed to a single, zero-mean-stress S-N curve (equivalent to R = -1).

The Goodman Fit defines the relationship between mean and alternating stress levels. This rule states that the fatigue life at alternating stress σ_a and mean stress σ_m is equal to the fatigue life at an equivalent zero-mean-stress alternating stress state of σ_e through the relation:

$$\sigma_a = \sigma_e \left[1 - \frac{\sigma_m}{\sigma_u}\right]^c \quad , \tag{10}$$

where σ_u is the ultimate strength of the material. Variations on this equation replace the ultimate strength of the material with the yield stress, or various fractions and/or combinations of the ultimate strength and yield stress. Usually the exponent c is taken to be equal to one, but other values are often used to improve the fitting characteristics. The form chosen for a particular material is usually determined using a best-fit algorithm.

Crack Propagation Model

A generalized crack propagation model was proposed by Forman et al.[7] This formulation takes the following form:

$$\frac{da}{dn} = \frac{C(1 - R)^m \Delta K^n (\Delta K - \Delta K_{th})^p}{[(1 - R) K_c - \Delta K]^q} \quad , \tag{11}$$

where da/dn is the crack propagation rate, ΔK is the change in the stress intensity factor K at the crack tip for the n^{th} cycle, and C, m, n, p, q, ΔK_{th} and K_c are material constants. The equation reduces to traditional formulations via the specialized values shown in Table I. In this table, m_w is a material constant. This formulation has been fit to a selected set of materials in Forman et al.[8]

Table I. Specialized Values for the Forman Crack Growth Model.

Constitutive Relationship	Exponent		
	m	p	q
Paris	0	0	0
Forman	0	0	1
Walker	$(m_w - 1)\, n$	0	0

WOOD

The *Wood Handbook*[9] is a general reference for the structural properties of solid wood. Wood is not a single material; rather, it includes many species with a wide range of mechanical properties and densities. Density variations range over an order of magnitude, from approximately 96 kg/m^3 (6 lb/ft^3) to 960 kg/m^3 (60 lb/ft^3). In general, the mechanical properties of wood, moduli and strength, are proportional to density because the basic organic material is essentially the same in all species. The design flexibility of wood is obvious. Low-density species, e.g. balsa wood, can be used as the core for sandwich panels where stiffness and buckling resistance must be accomplished with a minimum weight design. And, high-density species, e.g., Douglas fir, are used for the blade skin and structural stiffeners where high strength is essential.[3]

General Properties

Mechanical Properties

The mechanical properties of wood are influenced significantly by a number of variables. As noted above, moisture content is the most significant. The *Wood Handbook*[9] presents a general empirical relationship that characterizes the changes in mechanical properties with moisture content. This relationship is for "clear" wood at approximately 20°C. The mechanical property P

(i.e., the various anisotropic moduli and strength properties) is related to the moisture content M (in percent by weight) by the following equation:

$$P = P_{12}\left[\frac{P_{12}}{P_g}\right]^{\left(\frac{M-12}{M_p-12}\right)} = P_{12}\,[K]^{\left(\frac{M-12}{M_p-12}\right)} \quad , \tag{12}$$

where P_{12} is the property at 12 percent moisture content, M_p is the moisture content at which changes in the property first occur as the wood is dried, and P_g is the property (in the green condition) for all wood moisture contents greater than M_p. M_p varies between 18 and 21 percent for most wood varieties. And the property P varies on the order of ± 20 percent for moduli and up to 35 percent for strength. The ratio of P_{12} and P_g, K, is a constant for a given wood and property. The adjustment of physical properties for moisture content is also covered by standards ASTM D 245 and 2915.

The mechanical properties of wood are also a function of temperature, time-at-load and sample volume. At constant moisture content and below about 150°C, mechanical properties are approximately linearly related to temperature, with the properties decreasing as the temperature increases. A change of 50°C from 20°C can produce as much as 50 percent change in modulus and, typically, a 20 or 30 percent change in strength. Time at load can increase strain by approximately 100 percent in a year's time, and decrease strength by 50 percent relative to properties determined in short-term tests.

Grading

Wood is a natural material. Thus, natural variations within a given species are common and are important to the design of structures made from wood. To obtain a consistent set of mechanical properties, wood is typically graded by visual inspection. This qualitative measure of the grain structure in a given piece (batch) of wood has proven to be a good indicator of the quality of its mechanical properties. The *Wood Handbook*[9] provides a detailed description of a typical visual grading system.

A quantitative grading system for grading veneer sheets was developed by Jung.[10,11] In this system, an acoustic wave (a 50 kHz wave was used in these studies) is passed along the length of the sheet [2.44 m (8 ft.)]. The transit time is then used to estimate the quality of veneer sheet. While the transit time is primarily a function of sheet's modulus, this measurement also reflects grain slope and knots, which can significantly reduce the quality of a veneer sheet. Gougeon Brothers, Inc.[3] has used this system successfully for grading the veneers they use in the construction of their laminated wood blades.

Laminated Wood

The techniques for manufacturing wooden wind turbine blades were drawn from the aircraft and boating industries. The process uses a laminated wood manufacturing technique to create a wood composite from sheet veneers [approximately 2.5 mm (0.1 in) thick] and epoxy. This process is

quite similar to that used for building hand-layup fiberglass composites structures. Wood veneers are first cut to size and then wetted with epoxy. They are then placed into a female mold. During the layup process, particular attention must be paid to the alignment of each sheet to ensure that the intra-layer joints are properly aligned. And, to ensure that the sheets lay flat in the mold, the curvature of each sheet is typically limited to a single axis of curvature. The entire stack of veneers are then cured as a single block that is typically vacuum bagged to remove excess air and to apply a uniform pressure to the stack as the bond is cured. In wind turbine applications, the resulting laminate is approximately 20 percent resin. This relatively high resin ratio is used to seal all the veneer's surfaces, thus controlling moisture, and to fill the voids and gaps that are typical of this relatively low-pressure manufacturing process.[3]

Although rather simplistic in concept, the design of a laminate structure is particularly complex in practice. Namely, the manufacturing process requires that each sheet be cut and trimmed to a shape that will fit precisely into the complex geometry of the mold. The shape of each piece of veneer is dictated by a number of considerations. First, each piece must lay properly in the veneer stack, i.e., the veneer's stiffness essentially restricts each piece to a single axis of curvature. Second, the inter-layer joints between pieces of veneer must be precisely aligned to ensure high-strength, fatigue-resistant joints. And, third, the joints must be staggered between the various layers to ensure that the final stack does not have joints occurring so close to one another that the structural integrity of the stack is compromised. Thus, sizing each piece of veneer becomes a difficult task in conformal geometry.

Moisture Content

The effects of moisture on a laminate-wood structure can be deduced by modifying Eq. 12.[3] For a weight fraction of epoxy that is given by ω_E, the moisture content of the wood is given by:

$$M = (1 + \omega_E) M_L \quad , \tag{13}$$

where M_L is the moisture content of laminate. Thus, Eq. 12 becomes:

$$P = P_{12} \left[\frac{P_{12}}{P_g} \right]^{-\left(\frac{(1+\omega_E)M_L - 12}{M_p - 12} \right)} = P_{12} \left[K \right]^{-\left(\frac{(1+\omega_E)M_L - 12}{M_p - 12} \right)} \quad . \tag{14}$$

The parameters contained in these two equations are described in the discussion of Eq. 12.

Attachments

As with most blades, the attachment of the blade root to the hub is critical to a reliable blade design. For wood blades, a bonded stud system has proven to be quite successful, see the discussion presented by Sutherland.[1]

Laminated Douglas Fir

In the U.S., laminated Douglas fir is the wood of choice for wood blades. Spera et al.[3] have characterized this material.

Moisture Content

The effect of moisture content on the mechanical properties of a laminated structure may be characterized using Eq. 14. In this equation, M_p equals 24 percent for Douglas fir, ω_E equals 0.22 and various values of the parameter K are summarized in Table II.

Table II. Typical Mechanical Property Ratios for Laminated Douglas Fir.

Property	K Values Used in Eq. 14.
Static tension parallel to grain	1.21*
Static tension perpendicular to grain	1.13*
Static compression parallel to grain	1.92*
Static compression perpendicular to grain	1.50
Static shear parallel to grain	1.07
Modulus of elasticity parallel to grain	1.05
Tension-tension fatigue parallel to grain	1.21
Compression-compression fatigue parallel to grain	1.92
Tension-compression fatigue parallel to grain	1.57

*Properties of clear Douglas fir.[9]

Fatigue Properties

A typical set of fatigue results of this study is shown in Fig. 3. Three important features in the fatigue design of these laminate structures are illustrated in this figure: grade, joint structure and size.

Grade

As illustrated in Fig. 3, the grade of the veneer does not imply consistent structural performance. In this case, a grade A veneer outperforms a grade A+ veneer. From a structural standpoint, the grading system quantifies the straightness of grain (grain distortions). As discussed above, the veneer can be graded either visually or mechanically. The acoustic technique provides a quantitative measure of the veneer's mechanical properties (modulus) and has proven to be the most consistent technique for grading veneers for wind turbine applications. This technique, to the extent possible, ensures a consistent structural grading of the quasi-static properties of the veneer coming into their process line, but not its dynamic (fatigue) properties. Thus, *the designer must always remember that wood is a natural material and can have subtle variations in properties that can only be detected with destructive testing.*

Joint Structure

The second effect illustrated in Fig. 3 concerns how two pieces of veneer in the same laminate layer are joined together. In this comparison, two internal joints are examined. In the first, called a butt joint, the edges of both veneers are square and they are simply butted up next to one another. In the second, called a scarf joint, the edges are tapered with complementary angles that permit the veneers to overlay one another in the joint.

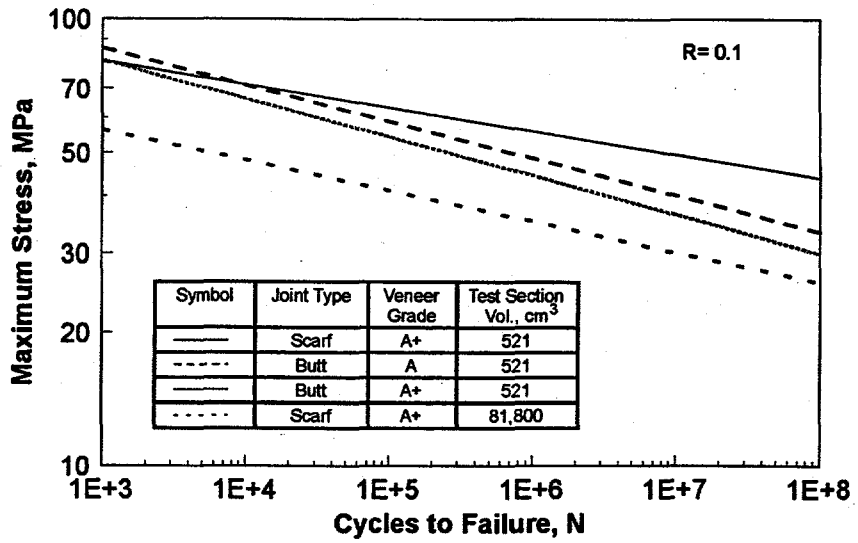

Figure 3. S-N Diagram for Douglas Fir/Epoxy Laminate.

Figure 3 illustrates that a scarf joint decreases the static and the low-cycle fatigue strength of a laminate structure. This measurement is in direct contradiction to what engineering judgment would indicate. Namely, the increased surface area in the joint created in the scarf does not translate into an increase in strength and fatigue resistance. In retrospect, several possibilities may be the cause of this reduced strength. The first is that the larger area of the scarf allows the veneer to out-gas during the layup process. Thus, the bond in the joint would contain a larger number of voids and significantly degrade the bond. Another possibility is that the joint is not aligned properly, which creates a thickness variation in the stack, namely the layer thickness is increased if the veneers are too close together (too much overlap) and is decreased when the veneers are too far apart (too little overlap). And, the thickness of the bond line will also be changed accordingly. At this time, the cause(s) of the reduced static strength and low-cycle fatigue resistance is unknown. These data also illustrate that high-cycle fatigue strength is increased by the scarf joint.

Size effects

As shown in this figure, wood, as with most natural materials, is subject to decrease in properties with increasing size. For the scarf joint, data from two sizes of samples are compared. In the first, the sample volume is 521 cm^3 (31.8 in^3) and in the second, it is 81,804 cm^3 (4992 in^3). Thus, the specimen volume has been increased by over two orders of magnitude. The data illustrate that the strength is decreased by approximately 20 percent from the first to the second. The size effect for the laminate strength σ_u may be characterized using:

$$\sigma_u = A V^{-B} + C \quad , \tag{15}$$

where V is the volume and A, B, and C are empirical constants. For the tensile strength of laminated Douglas fir, the values of these constants are 126 MPa (18300 psi), 0.320, and 56.2 MPa (8150 psi), respectively. The volume effect is typically less in compression than in tension.

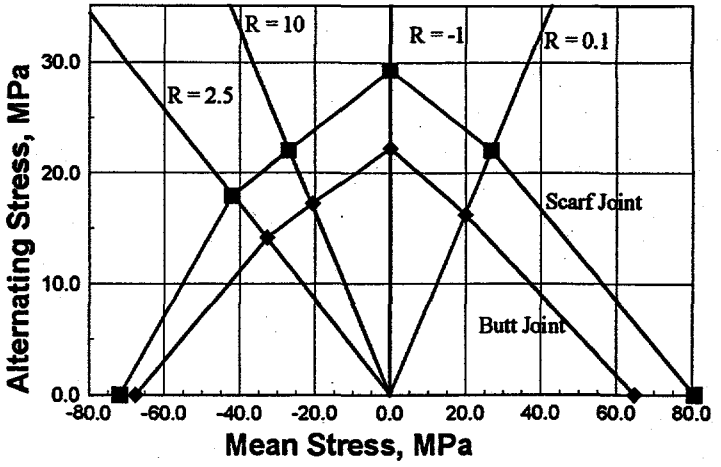

Figure 4. Goodman Diagram at 10^7 Cycles for Douglas Fir/Epoxy Laminate.

Goodman Diagram

The data contained in Fig. 3 and other data can be combined to form a Goodman diagram for the Douglas fir/epoxy laminate. Rather than show the entire diagram here, the partial diagram for 10^7 cycles is shown in Fig. 4. As shown in this figure, the diagram is approximately symmetric and, at 10^7 cycles, the scarf joint outperforms the butt joint. All of these data are for 521 cm^3 (31.8 in^3) test sections, a test temperature of 21°C (70°F) and the moisture content normalized to 6 percent.

Other Wood Laminates

Douglas fir is the material of choice for U.S. companies. However, other woods have been chosen and used successfully by other companies. Some of the woods that have been investigated include Khaya ivorensis (an African mahogany),[12] Swedish spruce and birch plywood,[13] Sitka spruce[14] and Baltic pine, popular, beech birch.[15]

METALS

Metals are the primary class of materials used to construct wind turbines. With the exception of the blades, most major components are constructed with ferrous alloys (primarily steel). Ferrous materials are favored by designers because there is extensive design experience with these materials from the rotating machine industry, they are relatively cheap to purchase and machine, and they can be fabricated easily using conventional practices. Moreover, they typically have a fatigue limit that permits the designer to design the turbine component to a stress level that essentially precludes failure in unjointed material.

In the early years of windmills and in the initial designs of modern wind turbines, most blades were constructed exclusive from metals. The modern turbine has forced turbine designers away from the relatively heavy metallic designs. Rather, they use composite materials to achieve the relatively lightweight designs that typify modern wind turbines. However, metallic alloys are the

materials of choice for making strong, reliable bolted joints. Thus, most current blade designs transition to aluminum or steel at the hub joint, debatably the most important joint in the entire turbine assembly.

From a material standpoint, this class of materials has been studied and extensively documented; e g., see Forman,[8] Fuchs and Stephens,[16] Boyer and Gall,[17] *Aluminum Standard and Data*[18] and Boyer.[19, 20]

Steel

Most of a wind turbine's structural components are constructed from ferrous alloys that are typically a variety of steel. From a fatigue standpoint, the drivers in the design of these materials are the joint structures used to combine the subcomponents of the wind turbine into its final structure. Joints, both mechanical and welded, create high stress concentrations,[21] introduce flaws and/or leave residual stresses that lead to failure.[22]

Discussions of these mechanisms are outside the realm of this report and are not discussed here. However, they are extremely important to building a reliable wind turbine and should not be overlooked in the design process.

Aluminum

The use of aluminum in wind turbine blades is an outgrowth of vertical-axis wind turbine (VAWT) technology. In this class of turbines, the blades do not require the twisted and tapered sections of horizontal-axis wind turbines (HAWTs) to achieve relatively high aerodynamic efficiencies. Moreover, through the use of extrusion technology, VAWT aluminum blades can be constructed quickly and relatively inexpensively.[23] Additional innovations in the manufacturing process also allow some variations in the aerodynamic cross sections of the blade through step tapering.[24] For these applications, the material of choice is 6063-T5 aluminum.

S-N Database

General properties for aluminum are provided in *Aluminum Standard and Data*[18] and Boyer.[19, 20]

VanDenAvyle and Sutherland[25] have developed a specialized database for extruded 6063-T5 aluminum. This material has a yield stress of 205 MPa (29.7 ksi) and an ultimate stress of 244 MPa (35.4 ksi). The fatigue database for this material contains approximately 100 fatigue data points obtained from bend specimens cycled at five alternating stress amplitudes and at four mean stress levels. The samples were tested to a maximum of 5×10^8 (500,000,000) cycles.

When the S-N data are mapped into the equivalent stress state using the Goodman rule, see Eq. 10, there are two distinct regions to the curve, see Fig. 5. Each segment may be fit with a straight line on a log-log plot of the form shown in Eq. 9; namely,

$$\log_{10} [\sigma_e] = C + b \log_{10} [n] \quad . \tag{16}$$

This segmented curve fit is shown in the figure as a solid line (labeled least squares curve fit). The respective confidence limits on the data, based on a statistical analysis for a Weibull fit to the variations about the least-squares fit, are also shown in the figure.

The aluminum data presented in Fig. 5 indicate that the aluminum has an apparent fatigue limit or at least a significant change in the slope of its S-N curve near 10^7 cycles. This break in the curve is particularly significant for characterizing the fatigue properties of aluminum for wind turbine applications.

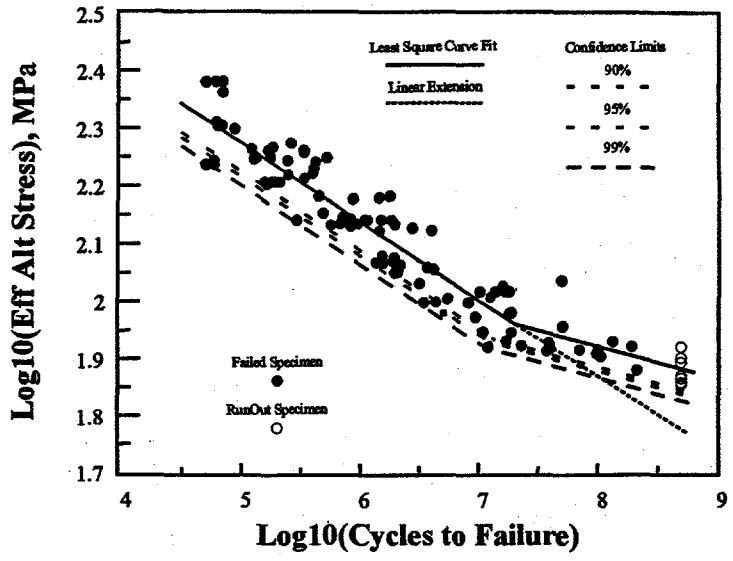

Figure 5. Normalized S-N Diagram for 6063-T5 Aluminum.

Spectral Loading

As noted above, typical S-N data are based on constant amplitude tests. The data plotted in Fig. 5 are no exception. As discussed by Mitchell,[26] if the aluminum specimens had been based on spectral loads instead of constant amplitude loads, the observed break in the data would probably disappear and the S-N data would follow a linear extension of the initial slope of the curve. This extension to the least-squares fit is shown in Fig. 5 as the short-dash line. Mitchell's argument is based on a crack-propagation view of the process. Under both classes of loading, a plastically deformed region surrounds the crack tip. Under high-stress constant-amplitude testing, each cycle is strong enough to overcome the residual stress field and, thereby, open and propagate the crack. However, under relative low-stress testing, the residual stresses restrict the crack opening displacement, and thereby, significantly reduce the growth rate of the crack. When spectral loads are applied, the relatively large components of the load spectra drive the crack into virgin material with little or no residual stresses. Thus, the crack growth rate is not restrained under low-stress loads, and the crack grows at the high stress rate.

Ashwill et al.[27] have investigated the influence of this extension on the fatigue life of a Sandia 34-m Test Bed.[28] In those calculations, the linear extension is shown to have little effect on the predicted service lifetime of this turbine. The fatigue exponent for metals (i.e., the reciprocal of b in Eq. 16) is typically relatively small, and the damage to the structure is governed primarily by the main body of the fatigue-load distribution. As the stress levels on this turbine are primarily above the stress threshold, see Fig. 5, the low stress region is of minor importance in the prediction of service lifetimes for this turbine, i.e., these cycles do not count when lifetimes are relatively short.

As with all designs, the finding that this region is not important for the prediction of service lifetimes in the Test Bed should only serve as a guide. In other turbines, this extension may be significant. *Thus, to remain conservative in the fatigue design of a turbine, the linear extension should be examined during the fatigue analysis of the turbine.*

Linear Crack Propagation Data Base

In addition to the development of S-N data, da/dn crack propagation curves have been developed for aluminum. Rolfe and Barsom[29] reported the general crack propagation properties of aluminum. The properties of 6063 aluminum are reported in Van Den Avyle and Sutherland,[25] Hatch, Van Den Avyle and Laing[30] and Warren and Pelloux.[31]

Sutherland and Schluter[32] have investigated this analysis technique to predict crack propagation in an aluminum blade on the 34-m test Bed Turbine.[28] In this analysis, the crack growth rate for aluminum was taken to be the generalized form developed by Rolfe and Barsom,[29] see Fig. 6. Starting from a rather small crack of 0.025 mm (0.001 in), the crack will grow to critical length (essentially infinite growth rate) in less than 6 months, see Fig. 7. *Thus, this linear fracture analysis suggests that the service lifetime of this aluminum blade is relatively short once a crack is present.*

Veers and Van Den Avyle[33] have investigated the application of the constant amplitude data to spectral loading conditions. Using the constant amplitude data obtained by Van Den Avyle and Sutherland,[25] the behavior of 6065-T5 aluminum is characterized using Eq. 11 with the constants m, p and q set equal to zero. Predictions based on this model are then compared to crack propagation data obtained under spectral loads. They find

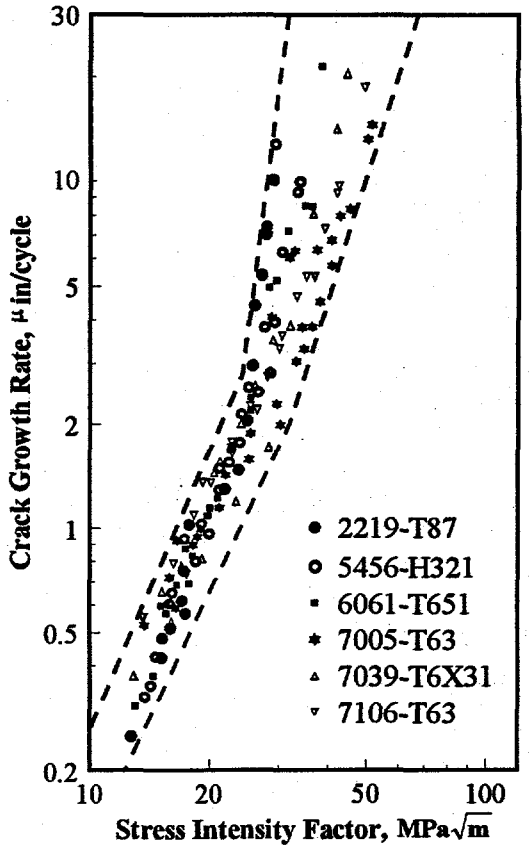

Figure 6. Fracture Mechanics Characterization for Aluminum Alloys.

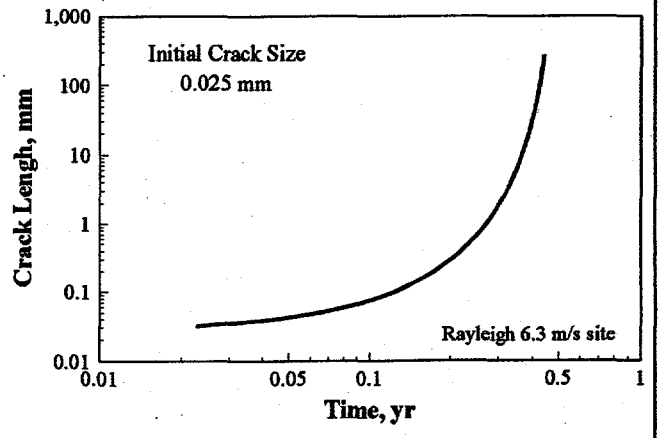

Figure 7. Crack Growth in an Aluminum Blade.

that linear models yield predictions that are not conservative for this material.

Gears

The AGMA has developed material properties and design practices for typical gear materials.[34, 35] A typical S-N diagram used by the AGMA for alloy steels case carburized to Rockwell C (R_c) 58-63 case hardness and 30-42 core hardness is shown in Fig. 8. The break in the curve, at approximately $2x10^6$ cycles in Fig. 8, is representative of a fatigue or endurance limit. The slope of the curve after the break is a 34.5 MPa (5 ksi) drop between $2x10^6$ to 10^8 cycles (see the discussion directly above). Additional S-N diagrams for gear materials are available in the literature and directly from gear manufacturers (proprietary data).

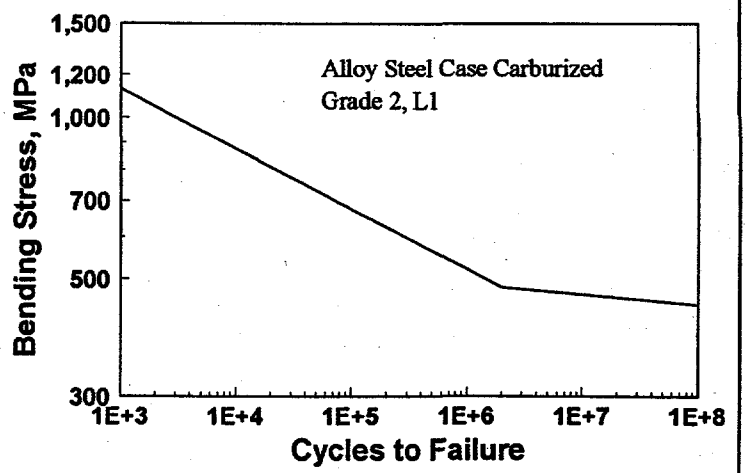

Figure 8. S-N Diagram for Carbonized Steel Gears.

FIBERGLASS COMPOSITES

Composites constructed with fiberglass reinforcements are currently the blade materials of choice for wind turbine blades. This class of materials is called simply fiberglass composites or fiber reinforced plastics (FRP). In turbine designs, they are usually composed of E-glass in a polyester, vinyl ester or epoxy matrix. Blades are typically produced using hand-layup techniques, but recent advances in RTM (Resin Transfer Molding) and pultrusion technology have blade manufacturers examining new procedures for increasing the quality of the final product and reducing manufacturing costs.

General references on designing with composite materials are provided in *Composites, Engineered Materials Handbook*[36] and Tsai and Hahn.[37] Mayer[38] describes the use of fiberglass composites for the design of wind turbine blades.

Databases

There are two main fiberglass composite databases for wind turbine applications. The first is the DOE/MSU database that has been developed in the U.S. by Mandell and Samborsky,[39] and the second is the European database. The latter is the compilation of the work of many researchers, that has been compiled as the FACT database by de Smet and Bach[40] and the recent compilation by Kensche.[2] The European database is best characterized as the study of a few materials in great

depth, and the former is best characterized as a study of many materials in not as much depth. Here, the DOE/MSU database will be used to illustrate data trends and the European database will be used to bring out the details that are important to the fatigue design of a wind turbine blade.

DOE/MSU

The DOE/MSU database was developed by Mandell et al. in a series of papers.[39,41-49] This database for E-glass composites contains over 6000 data points for 130 material systems. A high frequency database provides a significant data set for unidirectional composites to 10^8 cycles. Most of the data are presented in terms of maximum initial strain measured in the early stages of the test. The database explores such material parameters as reinforcement fabric architecture, fiber content, matrix materials and loading parameters (R values).

European Database

The European database is a compilation of data from many research groups. Most of these data was collected under the auspices of the European Commission (EC). The objective of the EC's program was to develop the basic information required to set design limits for rotor blades constructed with Glass Fiber Reinforced Plastics (GFRP). The compilation of these data is the FACT database.[40] A complete collection of the database, an evaluation of results and a detailed list of the references are provided in Kensche.[2] Only selected references from this database are discussed here.

Trend Analysis

As discussed by van Delft et al.[50] and used by many other authors, the S-N behavior of composite materials at a constant R value is typically described using either Eq. 6 or 9. Typically, Eq. 9 has been used to characterize the DOE/MSU database.[39] The European database is typically fit with Eq. 6.[40, 50]

Equation 9 was chosen to characterize the DOE/MSU database because the fit yields a value for C that is very close to 1. As discussed below, this property is extremely important when characterizing composite data, because normalization to the static strength may then be used to eliminate batch-to-batch material variation in the fatigue data.

The formulation shown in Eq. 9 has led to the *"ten percent" rule* that is typically used as a general rule-of-thumb for the tensile fatigue behavior ($R \cong 0.1$) of uniaxial composites.[51] Namely, the fatigue strength of the composite is reduced by ten percent by each decade of fatigue cycles, i.e., when C is one and b is one tenth (i.e., a fatigue exponent of 10). A similar rule-of-thumb for compressive fatigue behavior ($R \cong 10$) reduces the compressive strength by approximately 7 to 8 percent for each decade, i.e., when C is one and b is 0.07 or 0.08. This form is typically used for composites when comparing different material systems because it normalizes out variations in the static strength. Other typical values for the fatigue exponent m are 3 for welded steel and 6 for aluminum.

Both forms of the material representation have been used extensively to fit composite fatigue data and, as discussed later, they have important implications to damage calculations for spectral data.

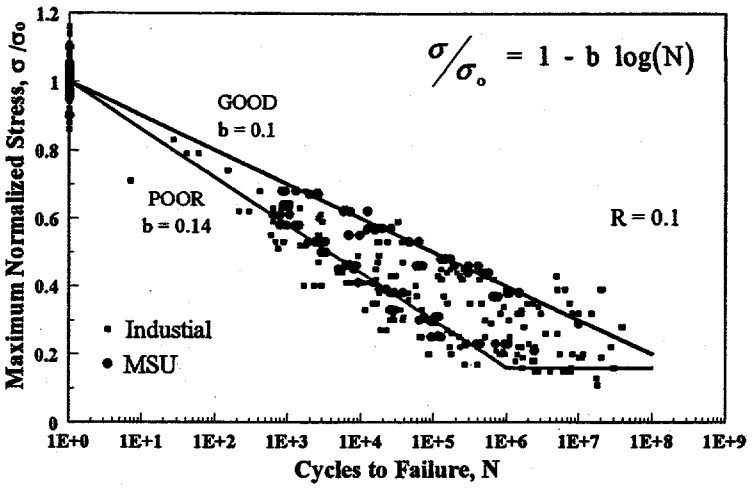

Figure 9. Extremes of Normalized S-N Tensile Fatigue Data for Fiberglass Laminates, R=0.1.

General Data Trends

A large number of data points from the DOE/MSU database are plotted in Fig. 9. These data are for fiberglass composites with at least 25 percent fiber in the loading direction tested at R = 0.1. When fit with Eq. 9, the good materials have a slope of 0.10 and the poor have a slope of 0.14. Thus, the good materials in this figure are approaching the best fatigue behavior that can be obtained for fiberglass materials in tensile fatigue (the ten percent rule for uniaxial composites at R = 0.1),[51] while the poor materials do not perform nearly as well. Indeed, the small appearing variation in the fatigue slope b produces significant differences in fatigue performance. As shown in the figure, at 20 percent of static strength, the good materials have almost 2.5 orders of magnitude longer life than the poor materials.

Figures 10 and 11 illustrate the trends for compressive and reverse fatigue. For compressive fatigue, the good materials have a slope of 0.07 and the poor materials have a slope of 0.11. For

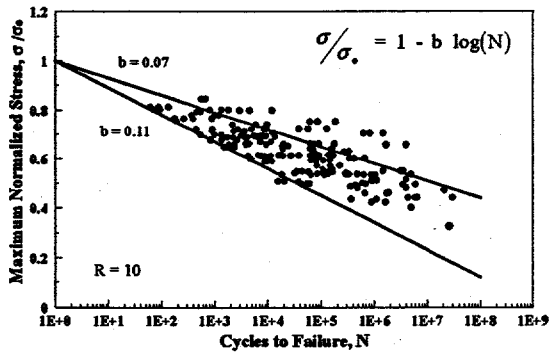

Figure 10. Extremes of Normalized S-N Compressive Fatigue Data for Fiberglass Laminates, R = 10. Normalized to the Ultimate Compressive Strength.

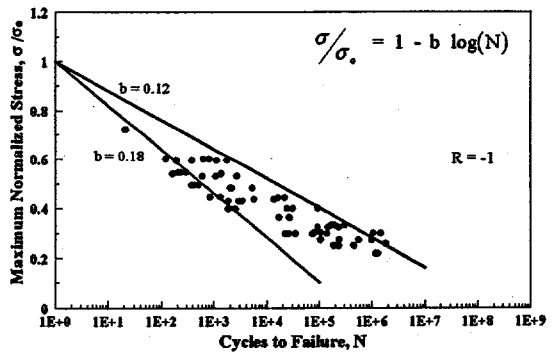

Figure 11. Extremes of Normalized S-N Reverse Fatigue Data for Fiberglass Laminates, R = -1. Normalized to the Ultimate Tensile Strength.

reverse fatigue, the slopes are 0.12 and 0.18, respectively.

Even when a family of laminates is tested, see Figure 12, similar behavior is observed in tension ($R \cong 0.1$), with slopes of 0.10 and 0.14 for the good and poor materials, respectively (The variation from good to poor materials is a direct result of the change in volume fraction from 31 percent for the good material to 54 percent for the poor material. This result is discussed in detail described in section entitled "Fiber Content" below.)

Thus, a major objective in the development of this database has been to sort out the differences between the good and the poor materials.

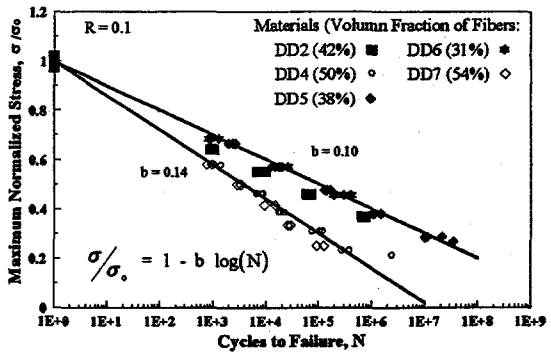

Figure 12. Extremes of Normalized S-N Fatigue Data for a Single Family of Fiberglass Laminates with 72% 0° Plies and 28% ±45° Plies, R = 0.1.

Fabric Architecture

The geometry of reinforcing fabrics plays a major role in static and fatigue properties. Woven glass-fabric composites typically show poorer tensile fatigue resistance than well-aligned, uniformly dispersed composite systems.[51] Samborsky et al.[48] give a comparison of static and fatigue properties for several types of E-glass fabric laminates with 0° plies. Ultimate tensile strength and elastic modulus are relatively insensitive to fabric type, but ultimate compressive strength is significantly lower for fabrics like A130 with a weave geometry that produces an out-of-plane curvature in the strands. Woven fabrics have about half the compressive strength of fabrics with straight strands. Mandell and Samborsky[39] note that the compressive fatigue resistance, when normalized by the ultimate compressive strength, is insensitive to fabric type or fiber content (straight-strand fabrics will also have significantly reduced compressive strength if the fibers become "wavy" during fabrication).

Typically, *the fabrics used in wind turbine application have either stitched or woven stand structures*, see Fig. 13.

A material that was investigated early in the development of this database was a stitched-triax material, i.e., the material contains 0° and ±45° layers that are stitched together with organic fibers at the factory to save handling costs during blade fabrication. Two laminate constructions with the same triax fabric were studied. The first had a 35 percent volume fraction of fibers and the second had a 40 percent volume fraction. Both laminates, called Material AA in the database,[39] behaved uniformly in the poor category, as did many other types of triax fabrics.[39] They are very important in this study because they provide an understanding of the basic difference between the best and worst materials in the entire database.

The essence of the results is that when the stitching is removed, the unstitched-triax behaves as one of the best materials. This observation is also true for an equivalent laminate (same layup schedule) constructed from unstitched 0° and ±45° layers. This result was explained with the aid of a detailed finite element analysis (FEA) of the local fiber stress in the composite near off-axis matrix cracks.[42,43,47] As the composite is loaded in tension, the matrix in the off-axis (45°) layers cracks (these cracks start forming at stress levels that are relatively low when compared to the static strength of the laminate). The FEA analysis of one of these cracked regions demonstrates that a local stress concentration factor of approximately 2.5 is generated in the 0° strands at the crossing of a 0° and a 45° layer. This large stress concentration is a direct result of the construction techniques used in the triax material. Namely, the organic fibers that are used to tie the various layers of the laminate together hold the glass fibers very close to one another, essentially touching. Under normal separation (obtained by not stitching the 0° and ±45° layers together), the stress concentration is approximately 1.4 to 1.7. Thus, the large local stresses produce early failure and uniformly poor fatigue behavior in the stitched triax material.

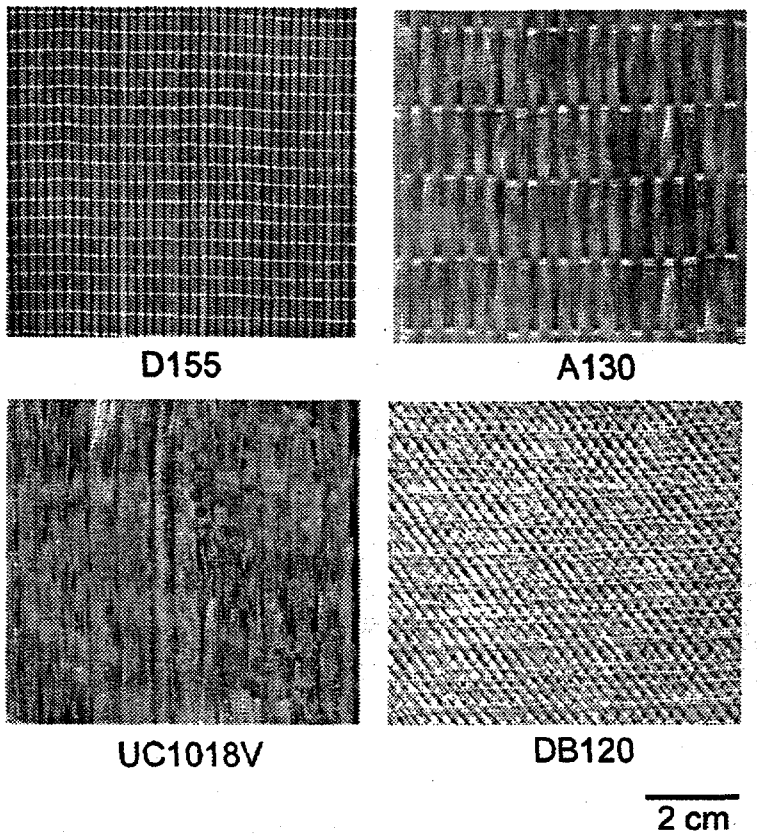

Figure 13. Dry Fabric Samples.

Fiber Content

The implication of the previous discussion is that behavior of composite systems will, in general, degrade as fiber content, is increased.[39] In earlier work, Mandell[51] found that many woven glass-fabric composites show poorer tensile fatigue resistance than the well-aligned, uniformly dispersed systems. Fig. 14 illustrates this behavior in several materials for fiber content, by volume, between approximately 30 and 60 percent. The materials cited in this figure are both cross-plied composite laminates, $[0/\pm45/0]_s$, (Materials AA and DD) and uniaxial laminates (Materials A130 and D155). As illustrated in Fig. 14a, material AA (stitched triax plies) has uniformly poor behavior, but when the separate, unstitched 0° and ±45° layers are used, there is a transition from

good to poor behavior that begins at an approximate fiber content of 35 percent (see Fig. 12). Note once again that the main difference between the AA triax and the DD laminate is that the 0° and ±45° layers in the AA material are stitched together.

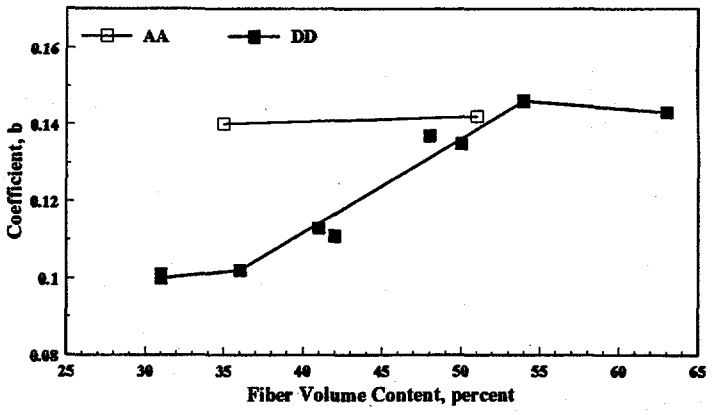

Figure 14a. Fatigue Sensitivity Coefficient for Various Fiber Contents in Fiberglass Laminates with 0° and ±45° Plies.

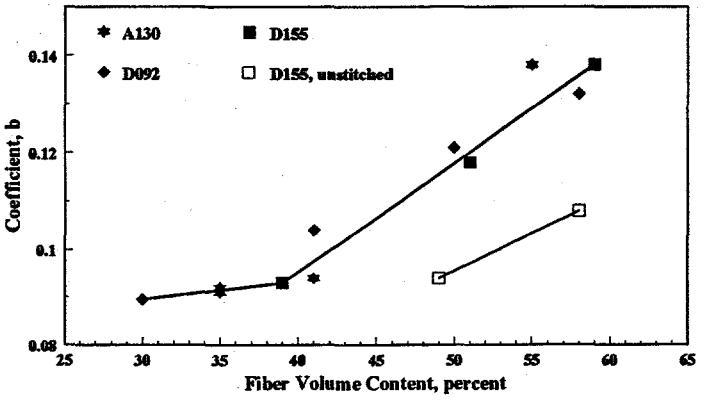

Figure 14b. Fatigue Sensitivity Coefficient for Unidirectional Fiberglass Laminates.

Figure 14. Fatigue Sensitivity Coefficient for Fiberglass Laminates as a Function of Fiber Content, at R = 0.1.

Similar data for unidirectional materials are shown in Figure 14b. As shown by data for the A130 (woven), D092 and D155 (loosely held together with organic fibers) composites, the optimum fatigue performance is achieved with a fiber content of approximately 40 percent. Moreover, as illustrated by unstitched D155 material data, if *all stitching*, be it relatively loose or otherwise, is removed, the progression from good to poor fatigue behavior is delayed to almost 50 percent fiber volume.

As discussed above, the origin of the sharp decrease in fatigue resistance as the fiber content increases apparently lies in a transition to a condition where the laminate fails in fatigue soon after the matrix cracks, usually along the stitching or weave cross-over.[39] When 45° plies are present, poor performance is observed if the 0° plies fail soon after the ±45° plies form matrix cracks. Good performance is associated with the 0° fiber wearing-out gradually, as occurs in the testing of a single strand of material.[39, 51]

Thus, the fiber separation is an important parameter for defining the fatigue behavior of composite laminate systems. And, although stitching makes fiber layers and bundles easier to handle in the manufacturing process, they degrade the fatigue behavior of the composite system.

Normalization

The above discussion uses normalized data to enable a relatively large number of laminate systems to be compared directly to one another. As the static tensile strength is approximately proportional to fiber volume fraction, the minimum fatigue coefficient b does not guarantee the optimum fatigue behavior. Rather, the increased strength offered by more fibers will offset a small amount of the decrease in the fatigue performance, depending on the design loads for the blade. However, *the strain-to-failure in fatigue is much lower (by a factor of approximately 2) for the materials with the poor behavior.*

Matrix Material

Three matrix materials are commonly used in the construction of composite blades for wind turbines. They are vinyl ester, polyester and epoxy. As reported in the DOE/MSU database[39] and the FACT database,[40] the matrix material has minimal effect on the static and fatigue properties of this class of composites because typical blade materials are primarily uniaxial. The various resin systems are compared in Fig. 15. These data are for tension fatigue (R=0.1) in an unstitched $[0/\pm45/0]_s$ composite. Similar results are obtained in both compressive and reverse fatigue.

Modulus Changes

The composite laminates that are typically used in wind turbine blades have very low strain-to-failure in the transverse direction. This characteristic implies that matrix cracking will be present in the off-axis ±45° plies of a laminated structure long before it fails. As shown in the MSU/DOE database,[39], the transverse ply's ultimate strain-to-failure is approximately 0.24 percent. This value translates to 0.39 percent strain in ±45° plies along the 0° direction of a $[0/\pm45]_s$ laminate. At a million cycles in tensile fatigue, the strain to failure in the 45's reduces to approximately 0.14 percent strain. The early loss of the matrix function in these layers translates into a decreasing laminate modulus.

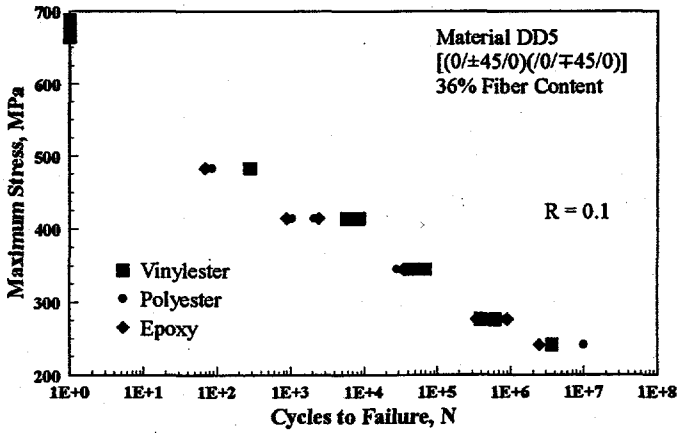

Figure 15. Effect of Matrix Material on Tensile Fatigue in a Fiberglass Laminate with 0° and ±45° Plies.

Figure 16 illustrates the drop in modulus for a cross-plied composite laminate, as a function of the normalized fatigue lifetime, i.e., n/N. As shown in this figure, the longitudinal modulus drops initially by 10 to 15 percent and then remains approximately constant for most of the laminate's lifetime. As the laminate approaches failure, the modulus drops precipitously.

Mandell and Samborsky[39] used standard laminated plate theory to estimate stiffness reduction as the off-axis plies are damaged. Their results, shown in Table III, are presented as the expected drop in laminate stiffness for several composite laminates. This prediction is based on the assumption that the transverse modulus E_T and the shear modulus G_{LT} of the ±45 layers decreases to 25 percent of the original value when their matrix material cracks. The 25 percent value was derived empirically and only applies to low cycle fatigue. *When empirical data are not available, the conservative approach to predicting stiffness reduction is to delete or severely decrease the properties of the matrix-dominated, off-axis plies, i.e., assume that the off-axis plies will be fully cracked almost immediately after the blade has been put into service.* Thus, E_T and G_{LT} for the off-axis plies are reduced to zero (or a slightly positive number).

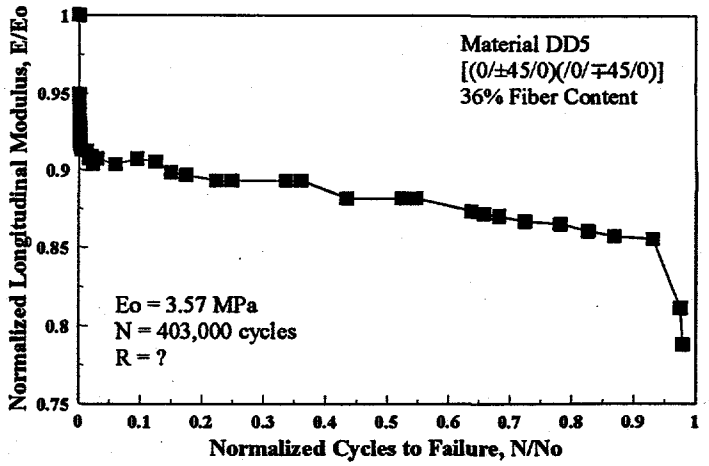

Figure 16. Reduction of Tensile Modulus in a Fiberglass Laminate with 0° and ±45° Plies Damaged in Tensile Fatigue.

Table III. Predicted and Measured Percent Decrease in Longitudinal Modulus due to Cracking of the ±45 Plies.

Layup	Volume Fraction of Fibers, percent	Decrease in Longitudinal Modulus percent	
		Predicted	Measured
$[0/\pm45/0]_s$	38	6.2	10
$[0/\pm45]_4$	36	16	10 - 20
$[\pm45/0/\pm45]_s$	36	31	31 -42

After the initial loss of modulus, the laminate continues to lose stiffness, see Fig. 16. This reduction should not be attributed to the cracking of the ±45 layers alone. Rather, the additional reduction is due to damage accumulation in the other layers of the laminate.

Mohamadian and Graham[52] have found similar results in composites constructed with chopped mat.

Predicting Service Lifetimes

Industrial Materials

Sutherland and Mandell[53] have demonstrated how the MSU/DOE database may be used to predict service lifetimes for wind turbine blades. Because the high-cycle portion of the database is primarily composed of data obtained from specialized material coupons, the requisite Goodman diagram is constructed using normalized coupon data. It is then de-normalized to typical industrial laminates for the analysis of service lifetimes. The procedures described in this reference should be used to ensure the blade material used in the construction of the wind turbine is the same as the blade material being analyzed. The analysis is based on material coupons, which perform close to the good line in Fig. 9 and will be non-conservative for poor laminates.

Database Comparison

A comparison of the Goodman Diagram from the two databases is shown in Fig. 17. Of particular significance in this comparison is that the diagrams for the MSU/DOE and the European (FACT) database are very similar to one another on the tension side (right side) of the diagram and very dissimilar to one another on the compression side (left side). This variation is a significant change in the form of the Goodman diagram. In particular, the MSU/DOE database yields a highly non-symmetric diagram with a strain to failure of 2.7 and 1.5 percent for tensile and compressive strengths, respectively.[44] This ratio of the tensile and compressive failure strains of 1.80 is significantly different from the European database which has a ratio of 1.33. Namely, the European database yields an approximately symmetric (about the zero mean-stress axis) Goodman diagram with strain-to-

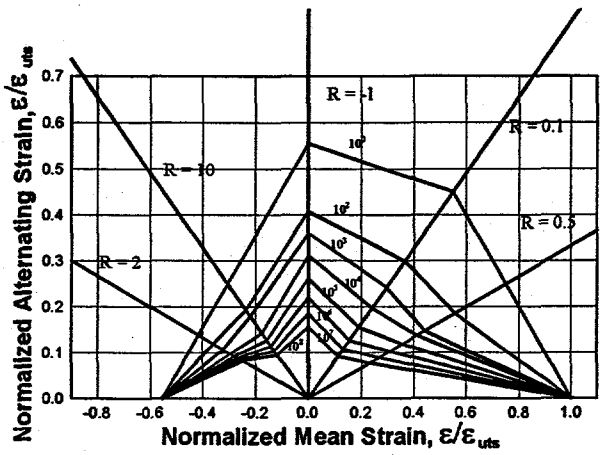

Figure 17a. Goodman Diagram based on the MSU/DOE Database.

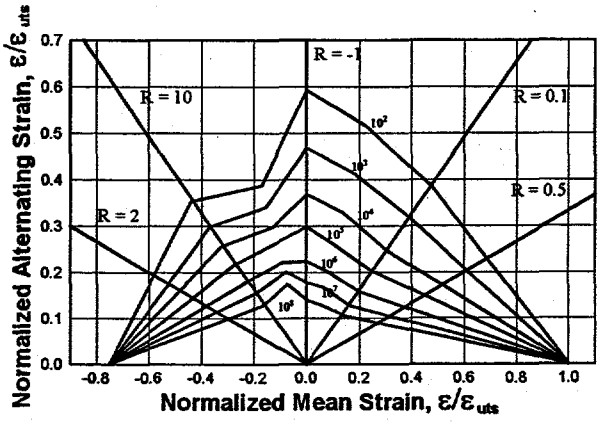

Figure 17b. Goodman Diagram Based on the FACT Database.

Figure 17. Goodman Diagrams for Fiberglass Composites.

failure of 2.58 and 1.94 in tension and compression, respectively.[40] A symmetric diagram implies that there are only small differences between tensile and compressive failures.

Although they could not prove it, Sutherland and Mandell[53] suggest that the discrepancy in the compressive failure-strain reflects the difference in compressive testing techniques. In particular, the compressive tests conducted for the MSU/DOE database used gauge sections with no lateral supports, whereas, the FACT database has a preponderance of data obtained from compression tests with lateral constraints. A sample of the more recent data from the MSU/DOE database illustrates that the ratio of the ultimate tensile to the ultimate compressive strain varies from 0.94 to 2.23 with an average value of 1.50.[39] Thus, differences in the databases can be attributed entirely to material variation. However, the differences in the testing techniques should not be discounted. Detailed comparisons of fatigue data from identical materials will be required to sort out the differences in the two databases.

When the two databases are compared on a non-normalized basis, the FACT data are found to contain a preponderance of the data that behave as the good material in the MSU database. Thus, the MSU/DOE database will predict a service lifetime that is equal to or shorter than that predicted by the FACT database.

Sutherland and Mandell[53] investigated the effect of these differences on predicted service lifetimes. Using the WISPER-protocol U.S. wind farm load spectrum,[54] the predicted service lifetimes for tensile failure were comparable (44.9 to 67.5 years based on the MSU/DOE and the FACT databases, respectively). However, for compressive failures, the predictions differed by approximately a factor of 5 (23.5 and 136 years, respectively).

Spectral Loading

Wind turbines are subjected to spectral loads that are unique to this structure. Test spectra have been proposed, and fatigue data on material behavior are being obtained. However, to date, these data are limited in extent. Van Delft et al.[50,55,56] have examined the differences between the response in fiberglass to constant and variable amplitude loading using the WISPER and the WISPERX spectrum.[57,58] Their experiments on a polyester fiberglass laminated with 0° and ±45° layers at approximately 32 percent fiber volume provide insight into using constant amplitude S-N data to predict service lifetimes under the spectral loads normally encountered by wind turbines.

WISPER vs. WISPERX

The WISPERX load spectrum is the WISPER spectrum with the small cycles removed. Damage estimates predict that the removal of the small cycles should have less than a 10 percent effect. However, the measured data indicated that a difference of the order of 50 percent (a factor of 2) is actually observed, see Fig. 18. These data imply that the low-amplitude cycles are more damaging than suggested by the constant amplitude S-N data.

Also the fatigue exponent b is changed from approximately 0.10 for the constant amplitude data to approximately 0.12 for the spectral data, a significant change (this exponent is based on the fit of the S-N curve for the number of the WISPER or WISPERX load sequences to failure).

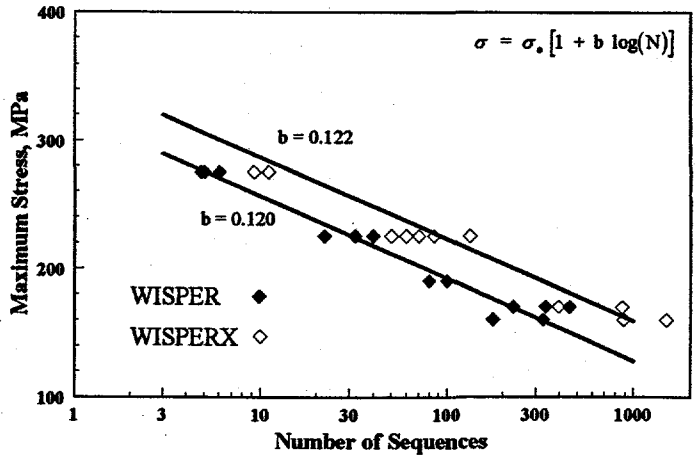

Figure 18. S-N Diagram for a Fiberglass Laminate with 0° and ±45° Plies, under WISPER Loading Conditions.

Predicted Service Lifetime

Van Delft et al.[50,56] have used the constant-amplitude European database to predict the response of composite coupons to the WISPER and the WISPERX loads. Lifetimes were predicted using Miner's rule and a power-law fit, see Eq. 4, to constant-amplitude S-N data for an R-value of a -1 (reverse loading). The data were expanded to a full Goodman diagram using a Goodman rule of the form shown in Eq. 10. *The predicted service lifetime is approximately two orders of magnitude higher than the measured lifetime*. However, when the S-N data were fit to a log-linear curve, Eq. 7, the predicted and measured service lifetimes were essentially the same, with the predicted service lifetime being slightly conservative.

In another study, Echtermeyer et al.[59] compared the predicted and measured fatigue life for several composite laminates to WISPERX spectral loads. These predictions of service lifetimes were based on a Goodman diagram constructed from S-N data for R-values of 0.1, -1 and 10. These data were fit best using a log-log representation. *In one laminate, the predictions agreed* with measured lifetimes. In two others, the prediction was a *factor of approximately 5 higher than the measured lifetime*. And in the final laminate, the predictions varied between a factor of 4 higher to a factor of 0.6 lower.

Thus, *the behavior of composites under typical wind turbine loads is not well understood* and is the subject of on-going research in various wind programs throughout the world. Based on the limited data discussed above and the data presented in Fig. 18, we can surmise that the low amplitude fatigue cycles are more damaging than indicated by the constant-amplitude S-N data.

Structural Details

The extension of coupon data to the behavior of full-size structural components is being studied by Mandell et al.[39,46,60-63] The results of their studies on such details as ply drops, local fiber content and transverse cracks are summarized in Table IV. The "knock-down" factor F in this

Table IV. Knock-Down Factors for Selected Structural Details in Tension and Compression for Approximately 70% 0° Materials.

DETAIL	SKETCH	KNOCK-DOWN FACTOR, F		
		A 130 Fabric	D155 Fabric	UC1018V Fabric
Simple Coupon (Straight Material)		1.0	1.0	1.0
Surface Indentation Tension, R=0.1 (V_f increased, thickness reduced by 25%)	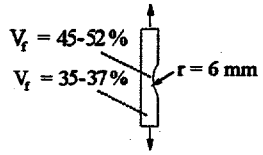	1.6	2.5	1.2
Surface Indentation Compression, R=10 (V_f increased, thickness reduced by 25%)	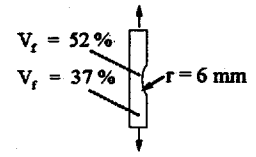	1.0	1.4	--
Locally Higher Fiber Content Tension, R=0.1 (2-90° Piles in center)	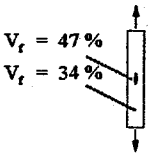	2.1	1.5	--
Locally Higher Fiber Content Compression, R=10 (2-90° Piles in center)	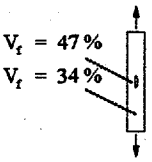	1.0	1.4	--
Exterior Cracked Transverse Tension, R=0.1 90° Patch		--	1.0	--
Double Interior 0° Ply Drop Tension, R=0.1	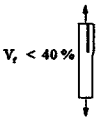	1.4	1.6	--

table is defined to be the ratio of the maximum cyclic strain (R = 0.1) of a uniform coupon to that of a structured coupon at one million (10^6) cycles; namely:

$$F = \frac{\text{Uniform Coupon Strain @ } 10^6 \text{ Cycles}}{\text{Structured Coupon Strain @ } 10^6 \text{ Cycles}} \quad (17)$$

Ply Drops

One common feature of blade structures is the use of ply drops to tailor the thickness of the composite structure to meet loads criteria while minimizing weight. In the detailed studies by Cairns et al.,[46,61] several configurations for the ply drops have been experimentally investigated and analyzed. As shown in Fig. 19, the ply drop may be internal (covered by at least one layer of fabric) or external.

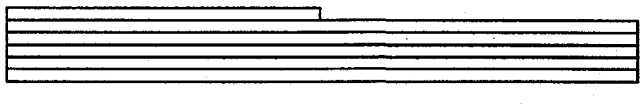

Figure 19a. External Ply Drop.

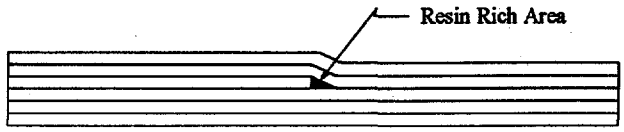

Figure 19b. Internal Ply Drop.

Figure 19. Typical Ply Drop Configurations.

The internal ply drop creates local stress concentrations that initiate failures. As shown in Table IV, these local stress concentrations can significantly reduce fatigue lifetimes. The investigation illustrated that *internal ply drops are less susceptible to delamination than external ply drops* and that for the same ply drops, *thicker laminates are better in resisting delaminations*. As indicated by an increased knockdown factor,[39] *dropping two plys in the same location is twice as harmful as dropping a single ply*, and that *feathering (i.e., staggering adjacent tows) or "Z-spiking" the ply will significantly decrease delamination growth rate* [Z-spiking consists of plunging some of the fibers from the ply drop edge into the adjacent layers (the z-direction)].

Locally Higher Fiber Content

As discussed above (in the section entitled "Fiber Content"), the fiberglass laminates typically used in wind turbine blades are *susceptible to significant degradation in their fatigue properties if fibers are forced very close to one another*. The effect is noted in the dependence in fatigue coefficient on fiber density shown in Fig. 14. *This effect also translates into local manufacturing defects, simulated by surface indentations and excess fiber layers*. As shown in Table IV, a surface indentation produces a knock-down factor of 2.5 for a local increase in fiber content from 35 percent to 47 percent in tension. In compression, the knock-down factor is 1.4 for a local increase in the fiber volume from 37 percent to 52 percent.

Transverse Cracks

In typical lay-ups of composite structures and especially for wind turbine blades, a high percent of the fibers is aligned with the primary load direction. Additional off-axis layers are added to prevent splitting and to increase shear properties. As discussed above, these off-axis layers are

typically more susceptible to fatigue damage. Ideally, these layers would split off from the underlying layers that carry the main loads without causing them to fail prematurely [the resulting failure of the cross section will be a relatively slow event that can be detected before catastrophic failure of the section (and the blade) occurs]. Thus, Table IV supports the concept that *no knock-down factor is required for the propagation of transverse cracks into uniaxial composites.* As discussed above, this factor is based on the assumption that fiber separation is adequate to prevent the fiber density effects discussed above.

Environmental Effects

As discussed by Kensche,[2] wind turbine blades are subjected to a hostile environment throughout their service lifetimes. The primary effects include ultra violet (UV) radiation; temperature fluctuations; rain, ice, humidity; thunderstorms/lighting; hailstones; erosion from sand particles; and extreme dryness in desert environments. A matrix-rich outer-layer of gel coat is typically applied to the blades to provide UV protection and to seal the exterior surface of the composite.

Kensche[2] summarizes the degradation of the mechanical properties of various laminate systems used in wind turbine blades and presents a general discussion of the topic. Bach[64] presents a general discussion of the influence of moisture on bolted joints in composite materials.

In terms of fatigue behavior for composite laminates in turbine applications, the three most important environmental factors are attacks on the matrix material by temperature, humidity and UV radiation. The gel coating offers good protection from UV radiation. Temperature alone is typically not an important environmental parameter because the turbine blades are designed for a specific range of operating temperatures and the laminate's matrix is chosen to meet those conditions [Differential thermal expansion can damage components of the wind turbine blade. However, as thermal expansion is more of a structural design problem than a material problem, it is not considered here.]. However, temperature and humidity combined to become the primary environmental factors that must be considered in the fatigue design of the blade. The discussions here will concentrate on these two environmental factors.

Equilibrium Moisture Content

Under time-varying environmental loads, Fick's law[2] may be used to predict moisture content. Several authors have used this technique to analyze the yearly cycle of environmental loads of temperature, humidity and rain on a turbine blade. Kensche[2] used this technique to analyze the moisture content of a blade subjected to a yearly cycle of cold-wet and warm-dry conditions. His predictions indicate that the moisture content will stabilize at 0.4 to 0.5 percent. Similar simulations have been conducted by de Bruijn[65,66] for the Dutch climatological cycle; see the discussion in section entitled "EN-WISPER Spectrum" below. For this set of conditions, the total moisture content is predicted to stabilize at approximately 0.25 percent. Measurements from a blade exposed to the Dutch environment for approximately four years agrees with the 0.25 percent prediction.

A question does arise concerning the use of the Dutch (northern European) climatological cycle for a general characterization of the behavior of composites under environmental loads. The Dutch cycle, and for that matter, a typical U.S. climatological cycle, is relatively benign. Turbines

designed for deployment in other regions, e.g. India, will have significantly higher environmental loads. Designers of advanced composite structures (e.g., those using carbon fibers) consider Vietnam's climatological cycle as their extreme case. Thus, a moisture content of of 0.4 to 0.5 percent is non-conservative for many applications.

Matrix Degradation

The matrix materials used in turbine blades are typically polymeric materials that absorb moisture from the humidity in the surrounding air and/or from water lying on their surfaces. The temperature governs the velocity of the diffusion process, and the humidity governs the moisture content. As the moisture content increases, the glass transition temperature, T_g, of the matrix is depressed, and the matrix will swell. Eventually, microcracks (crazing) may form in the matrix. Depending on the physical and chemical properties of the matrix (i.e., toughness, etc.), these changes may destroy the structural integrity of the laminate. This damage to the matrix has minimal effect on the tensile behavior of the laminate because the fibers are the primary load carrier. However, these effects are significant in compression and shear, where the matrix is the primary load carrier.

Property Degradation

Kensche[2] presents a detailed examination of the effects of absorbed moisture on the physical properties of a typical epoxy laminate system. In this set of data, the test specimens have been preconditioned using continuous hot-wet conditions. These conditions are 90 percent humidity at 45°C. Under these conditions, specimens reach equilibrium in approximately 120 days with moisture content between 0.4 and 0.5 percent.

When comparing the properties of moist and dry virgin specimens, the static tensile strength was essentially not affected by absorbed moisture (as one would anticipate). The static compressive strength was reduced by approximately one third and the interlaminar shear strength by slightly over ten percent.

Figure 20 compares the fatigue performance of wet and dry samples under reverse loading (R = -1). These data illustrate that the strain-to-failure for a given lifetime (number of cycles to failure) is reduced by 15 to 20 percent. With the larger value occurring in the low-cycle region.

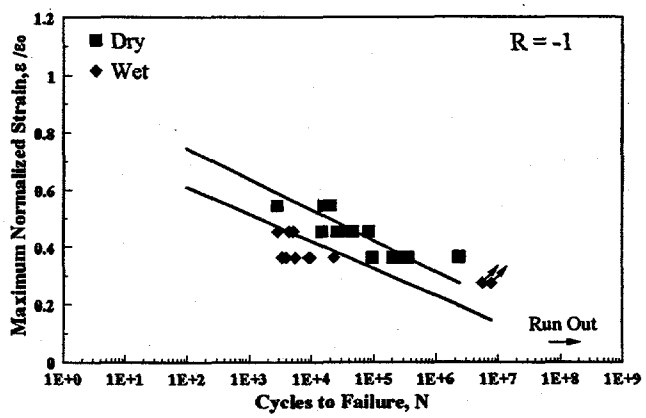

Figure 20. S-N Diagram for a Fiberglass Laminate with 0° and ±45° Plies, under Wet and Dry Environment Conditions.

Mandell[67] predicts similar results in compression tests of fiberglass coupons subjected to distilled water at 40°C for

approximately 190 days. Under these conditions, the polyester matrix has a weight gain of approximately 3 percent. The compressive strength of these coupons is reduced by 10 to 20 percent when tested at room temperature. When tested at 50°C, the compressive strength is reduced by 20 to 35 percent.

EN-WISPER Spectrum

As discussed above, many of these tests are based on pre-conditioning the samples in a hot-wet environment. However, wind turbine blades in the field undergo a series of environmental changes, typically on an annual cycle that both adds and removes absorbed moisture from the blade. To help quantify the effects of field environment, de Bruijn[65,66] and Joosse[68] have proposed a reference environmental spectrum. The spectrum is based on the annual Dutch climatological cycle, summarized and idealized (simplified) in Table V. The accelerated pre-conditioning cycle they proposed to simulate this climatological cycle is shown in Table VI. Both simulations and field measurements were used to validate that the accelerated cycle reproduced both the moisture profile and the moisture content.

Table V. Idealized Annual Climatological Cycle for the Dutch Environment.

Condition	Time, days	T, °C	ΔT, °C/hour	Relative Humidity, percent
Normal	228	10	5*	80
Hot	5.5	32	-5*	50
Frosty	22	-15	5*	85
Wet	109	8		100

*Rate of change of the temperature from the current to the next condition.

Table VI. Accelerated Climatological Cycle for the Dutch Environment.

Condition	Time, days	T, °C	ΔT, °C/hour	Relative Humidity, percent
Normal	105	18	50*	85
Hot	2.5	45	-50*	40
Frosty	10	-23	50*	100
Wet	49	16		100

*Rate of change of the temperature from the current to the next condition.

When tested, *the S-N data from samples that have been pre-conditioned by the EN-WISPER spectrum are not significantly different from non-conditioned specimens*; in contrast with the hot-wet pre-conditioned specimens discussion above. Joose[68] attributes this apparent discrepancy to a dominance of the test on the ambient conditions during the test. Implications of this observation are many. However, as noted by Joose, some test procedures have been called into question and require more study. Thus, the *pre-conditioned hot-wet samples do bound the*

problem, but the penalties in material performance they predict are probably too high for actual field conditions in Northern Europe and in most of the U.S. This may not be the case for India and Southeast Asia.

Effects of the Environment

At this time, environmental effects on composite turbine blades are not well understood, and are currently a subject of research, discussion and speculation. For instance, some studies of advanced composites for aircraft indicate that the daily maximum use temperature is more important than the average temperature. *Thus, current databases may yield non-conservative designs for environmental loads. And, the designer should use them only with extreme care.*

Comments

The design of composite materials for wind turbine blades has relied heavily on fiberglass technology. This material system has proven adequate to the task, even though it must withstand extremely large numbers of fatigue loads with varying amplitudes under extreme environmental conditions. Potential areas for increasing the performance of this system have been identified and are being pursued. In addition to increasing the performance characteristics of the materials system, an understanding of the influence of spectral and bi-axial loading on cumulative damage rules must be developed.[69] Also, design criteria for full-sized structures that are based on coupon data must be determined.

As blades become larger, stiffness considerations are becoming more and more important to the design. Fiberglass systems may not be able to meet these requirements within reasonable design constraints on weight. The obvious answer to this design issue is to introduce stiffer fibers, i.e., carbon fibers, into the composite system. Typically, carbon fiber designs have been too expensive for wind turbine applications. However, mixed fiber designs are currently under consideration and appear to be cost effective. These systems are not represented in the databases described above, but will need to be added. Specifically, the composite system with a mix of glass and carbon fibers will have to be addressed.

FATIGUE LIMIT DESIGN

The use of a fatigue limit for the fatigue analysis of structures is based on the observation that some metals have an essentially infinite life when tested at or below the value of their fatigue limit. Thus, the structural design is based on reducing the stress level at the highest load to the fatigue limit.

In terms of the S-N curve, an infinite life translates to a zero slope. Most materials do not have a true fatigue limit. However, many metals exhibit a significant reduction in the slope of their S-N curve as the number of cycles to failure gets very large. Figures 5 and 8 illustrate this behavior in aluminum and steel, respectively. For this class of behavior, a fatigue limit analysis can be conducted by assuming a quasi-fatigue limit that corresponds to the largest number of the cycles

the structure will have to bear. In Fig. 5, the quasi-fatigue limit would be between 60 and 80 MPa for 10^9 cycles; in Fig. 8 the limit occurs at approximately $2x10^6$ cycles.

The existence of a true or quasi fatigue limit is usually based on the experimental data obtained from constant amplitude fatigue tests. In many cases, when these materials are tested with variable amplitude loads, the initial slope of the S-N curve does not change as the number of cycles become very large, see the discussion of "Aluminum" above. *Because wind turbines are subjected to spectral loads, the use of constant-amplitude fatigue limit is probably not appropriate for most materials used in wind turbine structures.*

PARTIAL SAFETY FACTORS

The IEC has adopted a set of partial safety factors in IEC-61400-1[70] to account for the uncertainties and variabilities in material properties (and in loads). For material properties, the partial safety factors are included for the following: unfavorable deviations of the strength of material from the characteristic value; inaccurate assessment of the resistance of sections or load-carrying capacity of parts of the structure; uncertainties in the geometrical parameters; and uncertainties in the relation between the material properties in the structure and those measured by tests on control specimens. A discussion of partial safety factors and their application to wind turbine design is beyond the scope of this report and is not discussed here.

CONCLUDING REMARKS

Wind turbines are fatigue critical structures that require detailed analyses to ensure survival under normal operating conditions in a turbulent environment. While these designs are difficult, they are not impossible. The material research that has been conducted over the past few years provides the designer with the knowledge base required to address design problems with a high degree of confidence. The most significant advancement over this decade is the development of an extensive database for fiberglass composite materials. This database not only provides the designer with basic material properties, it provides guidance into engineering the material to achieve better performance without significantly increasing costs. Some questions have yet to be answered, but research is ongoing. The primary ones are the effects of spectral loading on fatigue behavior, scaling the properties of non-metallic materials from coupons to actual structures and environmental degradation of typical blade materials.

ACKNOWLEDGMENTS

In this article, I have drawn upon the work of many researchers. I wish to express my appreciation to them and to the many others who have made significant contributions to the understanding of fatigue in wind turbines. Due to space limitations, I have not listed all of the references pertaining to my subject. Rather, I have tried to hit the high points and provide readers with sufficient information to expand their reading list, as they deem necessary.

The author also wishes to offer particular thanks to a group of his technical associates who have reviewed this article, in whole or in part. Their constructive criticism has greatly enhanced this review article. Thanks to Henry Dodd, Craig Hansen, Don Lobitz, John Mandell, Kurt Metzinger, Walt Musial and Paul Veers.

Sandia is a multiprogram laboratory operated by Sandia Corporation, a Lockheed Martin Company, for the United States Department of Energy under contract DE-AC04-94AL85000.

REFERENCES

1. Sutherland, H.J., *On the Fatigue Analysis of Wind Turbines*, SAND99-

2. Kensche, C.W., ed., *Fatigue of Materials and Components for Wind Turbine Rotor Blades*, EUR 16684, European Commission, Luxembourg, 1996.

3. Spera, D.A., J.B. Esgar, M. Gougeon, and M.D. Zuteck, *Structural Properties of Laminated Douglas Fir/Epoxy Composite Material*, DOE/NASA Reference Publication 1236, DOE/NASA/20320-76, Cleveland, 1990.

4. *Handbook of Fatigue Testing*, S.R. Swanson, ed., ASTM STP 566, Philadelphia, 1974.

5. Osgood, C.C., *Fatigue Design*, Second Edition, Pergamon Press, New York, 1982.

6. Miner, A.A., "Cumulative Damage in Fatigue," *Trans. ASME*, Vol. 67, 1945, p. A159.

7. Forman, R.G., V. Shivakumar and J.C. Newman, *Fatigue Crack Growth Computer Program: "NASA/FLAGRO,"* NASA, JSC-22267, Houston, 1986.

8. Forman, R.G., *Derivation of Crack Growth Properties of Materials for NASA/FLAGRO*, NASA, Materials Branch Report 86-ES5-1, Houston, 1986.

9. *Wood Handbook: Wood as an Engineering Material*, Forest Product Laboratory, U.S. Dept. of Agriculture, Agriculture Handbook 72, Washington, 1987.

10. Jung, J., *Stress Wave Grading Techniques on Veneer Sheets*, Forest Products Laboratory, General Technical Report FPL-27, Madison, 1979.

11. Jung, J., "Properties of Parallel-Laminated Veneer From Stress-Wave-Tested Veneers," *Forest Products Journal*, vol. 32, no. 7, 1982, pp. 30.

12. Jamieson, P., "The Design of Wood Epoxy Wind Turbine Blades," *Eighth ASME Wind Energy Symposium*, D.E. Berg and P.C. Klimas, eds., SED-Vol. 7, ASME, 1989, p. 147.

13. Pedersen, M.U., and C.O. Clorius, *The Strength of Glued-in Bolts after 9 Years In Situ Loading*, Technical University of Denmark, DK9601314, NEI-DK-2303, 1995.

14. Stipe, C., W. Musial, M. Jenks, and S. Hughes, *Static Ramp and Compression-Compression Fatigue Testing of Sitka Spruce Specimens*, National Renewable Energy Laboratory, Golden, 1999.

15. Bonfield, P.W. I.P. Bond, C.L. Hacker and M.P. Ansell, "Fatigue Testing of Wood Composites for Aerogenerator Blades. Part VII, Alternative Wood Species and Joints", *Wind Energy Conversion*, B.R. Clayton, ed., Mechanical Engineering Publications Ltd., 1992, p. 243.

16. Fuchs, H.O., and R.I. Stephens, *Metal Fatigue in Engineering*, Wiley & Sons, New York, 1980.

17. Boyer, H.E., and T.L. Gall, eds., *Metals Handbook*, Desk Edition, American Society for Metals, Metals Park, Ohio, 1985.

18. *Aluminum Standard and Data, 1984*, Eighth Edition, The Aluminum Association, Washington, DC, 1984.

19. Boyer, H.E., ed., *Atlas of Stress-Strain Curves*, American Society for Metals, Metals Park, Ohio, 1985.

20. Boyer, H.E., ed., *Atlas of Fatigue Curves*, American Society for Metals, Metals Park, Ohio, 1985.

21. Peterson, R.E., *Stress Concentration Factors, Charts and Relations Useful in Making Strength Calculations for Machine Parts and Structural Elements*, Wiley Interscience Publication, New York, 1974.

22. Hoeppner, D.W., ed., *Fatigue Testing of Weldments, STP 648*, American Society for Testing and Materials, Philadelphia, 1977.

23. Alcoa Industries working with SNL engineers in mid 1970s: see, Kadlec, E.G., *Characteristics of Future Vertical Axis Wind Turbines*, SAND79-1068, Sandia National Laboratories, Albuquerque, NM, 1982.

24. Berg, D.E., P.C. Klimas, and W.A. Stephenson, "Aerodynamic Design and Initial Performance Measurements for the Sandia 34-m Diameter Vertical-Axis Wind Turbine," *Ninth ASME Wind Energy Symposium*, D. E. Berg, ed., SED-Vol. 9, ASME, 1990, p. 85.

25. Van Den Avyle, J.A., and H.J. Sutherland, "Fatigue Characterization of a VAWT Blade Material," *Eighth ASME Wind Energy Symposium*, D.E. Berg and P.C. Klimas, eds., SED-Vol. 7, ASME, 1989, p. 125.

26. Mitchell, M. R., "Fundamentals of Modern Fatigue Analysis," *Fatigue and Microstructure*, ASM Material Science Seminar, St. Louis, MO, 1978, American Society for Metals, 1979.

27. Ashwill, T.D., H.J. Sutherland, and P.S. Veers, "Fatigue Analysis of the Sandia 34-Meter Vertical Axis Wind Turbine," *Ninth ASME Wind Energy Symposium*, D. E. Berg, ed., SED-Vol. 9, ASME, 1990, p. 145.

28. Ashwill, T.D., D.E. Berg, L.R. Gallo, R.D. Grover, P.C. Klimas, M.E. Ralph, M.A. Rumsey, W.A. Stephenson, and H.J. Sutherland, "The Sandia 34-Meter VAWT Test Bed," *Proceedings of Wind Power '87*, American Wind Energy Association, SERI/CP-217-3315, 1987, p. 298.

29. Rolfe, S.T., and J.M. Barsom, "Fracture and Fatigue Control in Structures," *Applications of Fracture Mechanics*, Prentice-Hall, 1977, p. 244.

30. Hatch, P.W., J.A. Van Den Avyle and J. Laing, *Fatigue Crack Growth Automated Testing Method*, SAND89-0778 Sandia National Laboratories, Albuquerque, 1989.

31. Warren, A.S. and R.M. Pelloux, *Fatigue Behavior of 6063 Aluminum Alloy Extrusions for Wind Turbine Applications*, Final Report, SNL Contract No. 33-7708, MIT, Cambridge, 1990.

32. Sutherland, H.J., and L.L. Schluter, "Crack Propagation Analysis of WECS Components using the LIFE2 Computer Code," *Eighth ASME Wind Energy Symposium*, D.E. Berg and P.C. Klimas, eds., SED-Vol. 7, ASME, 1989, p. 141.

33. Veers, P.S., and J.A. Van Den Avyle, "Fatigue Crack Growth from Narrow-Band Gaussian Spectrum Loading in 6063 Aluminum Alloy," *Advances in Fatigue Lifetime Predictive Techniques*, ASTM STP 1122, M.R. Mitchell and R.W. Landgraf, eds., ASTM, Philadelphia, 1992, p. 191.

34. AGMA Standard, *Standard - Design Guide for Vehicle Spur and Helical Gears*, AGMA 170.01-1976, American Gear Manufacturers Association, Alexandria, VA, 1976.

35. AGMA Information Sheet, *Geometry Factors for Determining the Pitting Resistance and Bending Strength of Spur, Helical and Herringbone Gear Teeth*, AGMA 908-B89, American Gear Manufacturers Association, Alexandria, VA, 1989.

36. *Composites, Engineered Materials Handbook*, Vol. 1, ASM, T.J. Reinhart, Tech. Chair., Materials Park, OH, 1998.

37. Tsai, S.W., and H.T. Hahn, *Introduction to Composite Materials*, Technomic Publishing Co., Inc., 1980.

38. Mayer, R.M., ed., *Design of Composite Structures Against Fatigue: Applications to Wind Turbine Blades*, Mechanical Engineering Publications, United Kingdom, 1996.

39. Mandell, J.F. and D.D. Samborsky, *DOE/MSU Composite Materials Fatigue Database: Test Methods, Materials, and Analysis*, SAND97-3002, Sandia National Laboratories, Albuquerque, 1997.

40. De Smet, B.J., and P.W. Bach, *Database FACT: Fatigue of Composite for wind Turbines*, ECN-C-94-045, ECN, Petten, 1994.

42. Mandell, J.F., R.M. Reed Jr., and D.D. Samborsky, *Fatigue of Fiberglass Wind Turbine Blade Materials*, Contractor Report SAND92-7005, Sandia National Laboratories, Albuquerque, NM, 1992.

42. Mandell, R.M., J.F. Reed Jr., D.D. Samborsky and Q. Pan, "Fatigue Performance of Wind Turbine Blade Materials," *Wind Energy - 1993*, S. Hock, ed., SED-Vol. 14, ASME, 1993, p. 191.

43. Mandell, J.F., R.M. Creed Jr., Q. Pan, D. W. Combs and M. Shrinivas, "Fatigue of Fiberglass Generic Materials and Substructures," *Wind Energy - 1994*, W.D. Musial, S.M. Hock, and D.E. Berg, eds., SED-Vol. 15, ASME, 1994, p. 207.

44. Mandell, J.F., D.W. Combs and D.D. Samborsky, "Fatigue of Fiberglass Beam Substructures," *Wind Energy - 1995*, W.D. Musial, S.M. Hock and D.E. Berg, eds., SED-Vol. 16, ASME, 1995, p. 99.

45. Samborsky, D.D. and J. F. Mandell, "Fatigue Resistant Fiberglass Laminates for Wind Turbine Blades," *Wind Energy: Energy Week*, ASME/API, 1996, p. 46.

46. Cairns, D.S., J.F. Mandell, M.E. Scott, and J.Z. Macagnano, "Design Considerations for Ply Drops in Composite Wind Turbine Blades," *1997 ASME Wind Energy Symposium*, AIAA/ASME, W. Musial and D.E. Berg, eds., 1997, p. 197.

47. Shrinivas, M., *Three Dimensional Finite Element Analysis of Matrix Cracks in Multidirectional Composite Laminates*, M.S. Thesis, Dept. of Chem. Engr., Montana State University, 1993.

48. Samborsky, D.D., J.F. Mandell and D.S. Cairns, "Selection of Reinforcing Fabrics for Wind Turbine Blades," *1999 Wind Energy Symposium*, AIAA/ASME, 1999, p. 32.

49. Mandell, J.F., D.D. Samborsky and H.J. Sutherland, "Effects of Materials Parameters and Design Details on the Fatigue of Composite Materials for Wind Turbine Blades," *Proceedings of 1999 EWEC*, 1999, in publication.

50. Van Delft, D.R.V., G.D. de Winkel, and P.A. Josses, "Fatigue Behavior of Fibreglass Wind Turbine Blade Material Under Variable Amplitude Loading," *1997 ASME Wind Energy Symposium*, AIAA/ASME, W. Musial and D.E. Berg, eds., 1997, p. 180.

51. Mandell, J.F., "Fatigue Behavior of Short Fiber Composite Materials," *The Fatigue Behavior of Composite Materials*, K.L. Reifsnider, ed., Elsevier, 1991, p. 232.

52. Mohamadian, H.P., and I.J. Graham, "Stiffness Degradation In Unidirectional + Chopped Mat E-Glass Fiber/Polyester and Vinylester Composite Laminates," *Tenth ASME Wind Energy Symposium*, D.E. Berg and P.S. Veers, eds., SED-Vol. 11, ASME, 1991, p. 55.

53. Sutherland, H.J., and J.F. Mandell, "Application of the U.S. High Cycle Fatigue Data Base to Wind Turbine Blade Lifetime Predictions," *Wind Energy: Energy Week*, ASME/API, 1996, p. 85.

54. Kelley, N.D., "A Comparison of Measured Wind Park Load Histories With The WISPER and WISPERX Load Spectra," *Wind Energy 1995*, Musial, Hock and Berg, eds., SED-Vol. 16, ASME, 1995, p. 107.

55. Van Delft, D.R.V., P.A. Joosse and H.D. Rink, "Fatigue Behavior of Fibreglass Wind Turbine Blade Material at the Very High Cycle Range," *Proceedings of EWEC '94*, 1994, p. 379.

56. De Winkel, G.D., and D.R.V. Van Delft, *Fatigue Behavior of Glass Fibre Reinforced Polyester for Wind Turbine Blades; Part 2: Fatigue Behavior under the WISPER and WISPERX Variable Amplitude Loading*, Stevin Report 6-96-20, Delft University of Technology, Delft, The Netherlands, 1996.

57. Ten Have, A.A., *WISPER and WISPERX: Final Definition of Two Standardized Fatigue Loading Sequences for Wind Turbine Blades*, NLR-TP-91476U, National Aerospace Laboratory NLR, Amsterdam, the Netherlands, 1992.

58. Ten Have, A.A., "WISPER and WISPERX: A Summary Paper Describing Their Backgrounds, Derivation and Statistics," *Wind Energy - 1993*, S. Hock, ed., SED-Vol. 14, ASME, 1993, p. 169.

59. Echtermeyer, A.T., C. Kensche, P. Bach, M. Poppen, H. Lilholt, S.I. Andersen and P. Brøndsted, "Method to Predict Fatigue Lifetimes of GRP Wind Turbine Blades and Comparison with Experiments," *Proceedings of the European Union Wind Energy Conference*, Göteborg, Sweden, 1996, p. 907.

60. Mandell, J., D. Samborsky and D. Cairns, "Advanced Wind Turbine Blade Structure Development Program at Montana State University," *1997 ASME Wind Energy Symposium*, AIAA/ASME, W. Musial and D.E. Berg, eds., 1997, p. 189.

61. Mandell, J., D. Samborsky, M. Scott and D. Cairns, "Effects of Structural Details on Delamination and Fatigue Life of Fiberglass Laminates," *1998 ASME Wind Energy Symposium*, AIAA/ASME, W. Musial and D.E. Berg, eds., 1998, p. 323.

62. Cairns, D., D. Haugen, J. Mandell and D. Samborsky, "Fracture of Skin/Stiffener Intersections in Composite Wind Turbine Structures," *1998 ASME Wind Energy Symposium*, AIAA/ASME, W. Musial and D.E. Berg, eds., 1998, p. 334.

63. Mandell, J.F., D.D. Samborsky, D.W. Combs, M.E. Scott and D.S. Cairns, *Fatigue of Composite Material Beam Elements Representative of Wind Turbine Blade Substructure*, NREL/SR-500-24379, National Renewable Energy Laboratory, Golden, CO, 1998.

64. Bach, P.W., *Fatigue of Stud Joints for GFRP Wind Turbine Blades*, ECN-C95-117, ECN, Petten, the Netherlands, 1995.

65. De Bruijn, J.C.M., J.A. ter Laak and C.A.M. van den ENDE, "EN-WISPER," *Proceedings of the IEA Third Symposium of Wind Turbine Fatigue*, IEA, Implementing Agreement for a Programme of Research and Development on Wind Energy Conversion Systems - Annex XI, 1994, pp. 55.

66. De Bruijn, J.C.M., *EN-WISPER: Environmental Influence on the Fatigue Behavior of Wind Turbine Rotor Blades*, 50950-KIM 95-9313, KEMA, Arnhem, 1995.

67. Mandell, J.F., Montana State University, Bozeman, personal communication to the author.

68. Joosse, P.A., "EN-WISPER: Research Overview and Consequences," *Proceedings of the IEA Third Symposium of Wind Turbine Fatigue*, IEA, Implementing Agreement for a Programme of Research and Development on Wind Energy Conversion Systems - Annex XI, 1996, p. 87.

69. Joose, P.A. and D.R.V. van Delft, "Has Fatigue Become a Wearisome Subject?," *Proceeding of the European Union Wind Energy Conference*, Göteborg, Sweden, 1996, p. 902.

70. *Wind Turbine Generator systems - Part 1: Safety Requirements*, IEC 61400-1, prepared by IEC-TC88, 1998.